Available online at www.sciencedirect.com
ScienceDirect
Journal of Sound and Vibration 317 (2008) 898–917
JOURNAL OF SOUND AND VIBRATION
www.elsevier.com/locate/jsvi

Dynamic buckling of shallow pin-ended arches under a sudden central concentrated load

Yong-Lin Pi, Mark Andrew Bradford*

Centre for Infrastructure Engineering and Safety, School of Civil and Environmental Engineering, The University of New South Wales, Sydney, Australia

Received 18 April 2007; received in revised form 22 January 2008; accepted 21 March 2008
Handling Editor: L.G. Tham
Available online 12 May 2008

Abstract

When a shallow arch is subjected to an in-plane load that is applied suddenly, the arch will oscillate about an equilibrium position due to the kinetic energy imparted to the arch by the sudden load. If the suddenly applied load is sufficient large, the motion of the arch may reach an unstable equilibrium position, leading to dynamic buckling of the arch. This paper presents a study of the dynamic in-plane buckling of a shallow pin-ended circular arch under a central radial load that is applied suddenly with infinite duration. The method of conservation of energy is used to establish the criterion for dynamic buckling of the shallow pin-ended arch and analytical solutions for the lower and upper dynamic buckling loads of the arch under this sudden central load with infinite duration are obtained. It is found that the dynamic buckling loads of a shallow pin-ended arch under a sudden central load with infinite duration are lower than its static buckling loads, and that the dynamic buckling load increases with an increase of a dimensionless arch geometric parameter that is introduced. The effect of static preloading on the dynamic buckling of a shallow pin-ended arch is also investigated. It is found that the pre-applied static load decreases its dynamic buckling loads, but increases the sum of the pre-applied load and the dynamic buckling load.

1. Introduction

When an in-plane load is applied suddenly to a shallow circular arch that is fully braced laterally (Fig. 1), the load will impart kinetic energy to the arch and will cause the arch to oscillate about an equilibrium position. If this suddenly applied load is sufficiently large, the arch may reach an unstable equilibrium position, which may then induce dynamic buckling of the arch.

Investigations of the dynamic buckling of shallow arches have concentrated on sinusoidal arches under loads distributed as half-sine waves [1–8]. In these studies, sine series methods were used and the coupling between the normal and axial deformations was not considered. Ignoring this coupling may be valid for very shallow sinusoidal arches. However, the coupling between the radial (normal) and axial displacements in a

*Corresponding author.
E-mail address: m.bradford@unsw.edu.au (M.A. Bradford).

0022-460X/$ - see front matter © 2008 Elsevier Ltd. All rights reserved.
doi:10.1016/j.jsv.2008.03.037

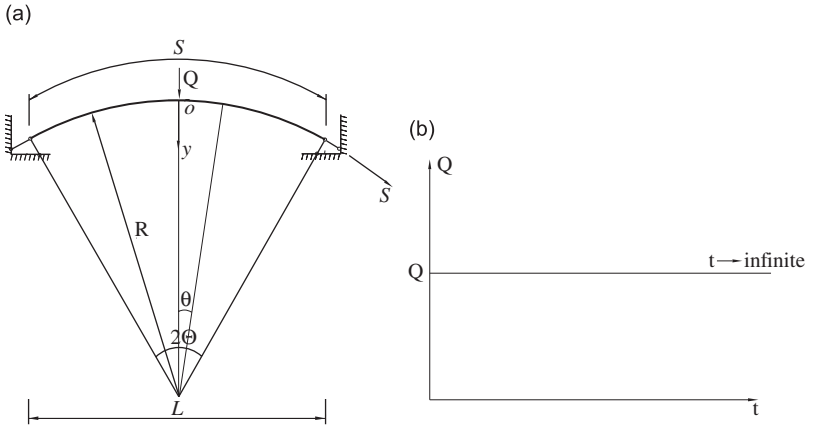

Fig. 1. Pin-ended shallow arch: (a) pin-ended arch and (b) sudden load with infinite duration.

circular shallow arch should not be ignored, particularly when exact closed form solutions are sought. Gjelsvik and Bodner [9] investigated the static instability of fixed shallow circular arches with a rectangular solid cross-section subjected to central point loading using an energy method, and approximate solutions were obtained. Schreyer and Masur [10] presented an accurate analysis of shallow circular arches and derived analytical solutions for static buckling, but their analysis was limited to fixed arches with a rectangular solid section. Dickie and Broughton [11] used a series method to study the static buckling of shallow circular pin-ended and fixed arches. Their study was also confined to rectangular solid cross-sections and only approximate numerical solutions were obtained. Pi et al. [12] obtained exact solutions for the in-plane static nonlinear buckling of circular arches with an arbitrary cross-section that are subjected to a radial load distributed uniformly around the arch axis, while Bradford et al. [13] performed an exact analysis for the in-plane static nonlinear buckling of circular arches with an arbitrary cross-section that are subjected to a central concentrated radial load. It was found that the structural behaviour of shallow arches becomes quite nonlinear under large loads and that the coupling between the radial and axial deformations is significant when predicting the structural behaviour of shallow arches. Hence, the effects of this nonlinearity on the in-plane buckling and the coupling between the radial and axial deformations needs to be considered in the analysis. Matsunaga [14] used the method of power series expansion of the displacement components to investigate the free vibration and dynamic stability of circular arches and presented an approximate theory for the dynamic buckling loads of shallow circular arches. Huang et al. [15] obtained series solutions in conjunction with a matrix analysis for the dynamic buckling of shallow circular arches including shear deformation. It was found that the accuracy of the results depended on the number of elements and on the number of terms in the series solutions. Kounadis et al. [16] performed a comprehensive nonlinear stability analysis for a one-degree-of-freedom arch and established its dynamic snap-through buckling strength under impact loading. Levitas et al. [17] used Poincaré-like simple cell mapping to present a study of the global dynamic stability of a shallow elastic arch that is subjected to uniform constant radial loading. Pinto and Gonçalves [18] investigated a strategy for the active nonlinear control of the oscillation of a shallow arch-like simply supported buckled beam in order to prevent dynamic instability.

It is known [1–8] that three different methods can be used successfully for determining the critical conditions for the dynamic stability of dynamically loaded elastic structures. The first method uses numerical solutions of the equations of motion of the structural system for various values of the load parameter to obtain the response of the system [1,2]. The load parameter at which there exists a large change in the response is considered as the critical one. The second method uses the total energy phase plane of a structural system [3]. Critical conditions are related to the characteristics of the system's phase plane, and the emphasis is on establishing sufficient conditions for stability and for instability. The third method is based on the principle of energy conservation [4], and so it can only be applied to a conservative system. The major merit of the third method is that it is devoted to finding the criterion which allows the dynamic buckling load to be determined without actually having to solve the equations of motion. Kounadis et al. [16,19,20] further developed energy

and geometric methods, performed a number of investigations of the nonlinear dynamic buckling of autonomous systems, and proposed useful dynamic buckling criteria based on an energy consideration. They studied the nonlinear dynamic buckling of autonomous non-dissipative N-degree-of-freedom systems [20], established dynamic instability criteria using characteristic distances associated with the geometry of the zero level total potential energy, and demonstrated the reliability and efficiency of the criteria by comparison with the results based on the Verner–Runge–Kutta scheme. In this paper, attention will be directed to using the third method to investigate the dynamic buckling of shallow arches. In some cases, a shallow arch may be subjected to a static load before the sudden load is applied. The behaviour of the shallow arch may become nonlinear under this static preloading and its dynamic buckling behaviour may be influenced by the static preloading, which also warrants an investigation.

The fourfold purposes of this paper are to investigate the in-plane dynamic buckling of a shallow pin-ended circular arch with a uniform cross-section that is subjected to a sudden central radial load which has an infinite duration (Fig. 1); to establish the criterion for the dynamic buckling of the arch using the principle of energy conservation; to obtain analytical solutions for the dynamic buckling of the shallow pin-ended arch under the sudden central load with infinite duration; and to study the effect of a static preloading on the dynamic buckling of the shallow pin-ended arch.

2. Differential equations of motion

The longitudinal normal strain ε at an arbitrary point on the cross-section of the circular arch can be expressed as the sum of the membrane strain ε_m and bending strain ε_b as [12]

$$\varepsilon = \varepsilon_m + \varepsilon_b \quad \text{with } \varepsilon_m = \tilde{w}' - \tilde{v} + \frac{1}{2}\tilde{v}'^2 \quad \text{and} \quad \varepsilon_b = -\frac{y\tilde{v}''}{R}, \tag{1}$$

where $()' = \partial()/\partial\theta$, θ is the angular coordinate, $\tilde{v} = v/R$, $\tilde{w} = w/R$, v and w are the radial and axial displacements of the centroid, R is the initial radius of the circular arch, and y is the coordinate of the point P in the principal axis system (Fig. 1).

It is assumed in this study that the dynamic response of the arch is undamped and that the rotatory kinetic energy can be neglected [4,17]. The Lagrangian $\mathscr{L}$ of the arch and load system can then be expressed as

$$\mathscr{L} = T - U, \tag{2}$$

where T is the kinetic energy given by

$$T = \frac{1}{2}\int_V m(\dot{v}^2 + \dot{w}^2)\,\mathrm{d}V = \frac{mA}{2}\int_{-\Theta}^{\Theta} R^3(\dot{\tilde{v}}^2 + \dot{\tilde{w}}^2)\,\mathrm{d}\theta, \tag{3}$$

where $\dot{()} = \partial()/\partial t$, t is the time, m is the mass density of the material, Θ is a half of the included angle of the arch, and U is the total potential energy of the arch and load system given by

$$U = \frac{1}{2}\int_{-\Theta}^{\Theta}\int_A ER\varepsilon^2\,\mathrm{d}A\,\mathrm{d}\theta - \int_{-\Theta}^{\Theta}\bar{\delta}(\theta)QR\tilde{v}\,\mathrm{d}\theta = \int_{-\Theta}^{\Theta}\left[\frac{1}{2}\left(EAR\varepsilon_m^2 + EI_x\frac{\tilde{v}''^2}{R}\right) - \bar{\delta}(\theta)QR\tilde{v}\right]\mathrm{d}\theta, \tag{4}$$

in which E is the Young's modulus, A is the area of the cross-section, I_x is the second moment of area of the cross-section about its major principal axis, and $\bar{\delta}$ is the Dirac delta function.

Substituting Eq. (1) into Eq. (2) and dividing Eq. (2) by the factor EAR leads to a dimensionless form of the Lagrangian as

$$\bar{\mathscr{L}} = \bar{T} - \bar{U} = \int_{-\Theta}^{\Theta}\left\{\frac{1}{2}\frac{mR^2}{E}(\dot{\tilde{v}}^2 + \dot{\tilde{w}}^2) - \left[\frac{1}{2}\left(\varepsilon_m^2 + \frac{r_x^2\tilde{v}''^2}{R^2}\right) - \frac{\bar{\delta}(\theta)Q}{EA}\tilde{v}\right]\right\}\mathrm{d}\theta, \tag{5}$$

where $r_x = \sqrt{I_x/A}$ is the radius of gyration of the cross-section about its major principal axis.

The equation of motion can be derived from Hamilton's principle which can be stated in the form

$$\int_{t_1}^{t_2} \delta\bar{\mathscr{L}}\,\mathrm{d}t = \int_{t_1}^{t_2} \delta(\bar{T}-\bar{U})\,\mathrm{d}t = 0 \quad \text{with } \delta\tilde{v}=\delta\tilde{w}=0 \text{ at } t=t_1,\ t_2 \text{ for } -\Theta\leqslant\theta\leqslant\Theta, \tag{6}$$

where t_1 and t_2 are arbitrary times.

Substituting Eq. (5) into Eq. (6), integrating by parts, and considering $\delta\tilde{v}=\delta\tilde{w}=0$ at $t=t_1,\ t_2$ leads to

$$\int_{t_1}^{t_2}\int_{-\Theta}^{\Theta}\left\{\left[\frac{r_x^2}{R^2}\tilde{v}^{iv}-\varepsilon_m\tilde{v}''-\varepsilon_m'\tilde{v}'-\varepsilon_m-\frac{\bar{\delta}(\theta)Q}{EA}+\frac{mR^2}{E}\ddot{\tilde{v}}\right]\delta\tilde{v}-\left[\varepsilon_m'-\frac{mR^2}{E}\ddot{\tilde{w}}\right]\delta\tilde{w}\right\}\mathrm{d}\theta\,\mathrm{d}t$$
$$+\int_{t_1}^{t_2}\left[\varepsilon_m\tilde{v}'\delta\tilde{v}+\frac{r_x^2}{R^2}(\tilde{v}''\delta\tilde{v}'-\tilde{v}'''\delta\tilde{v})+\varepsilon_m\delta\tilde{w}\right]_{-\Theta}^{\Theta}\mathrm{d}t=0. \tag{7}$$

Because the virtual displacements $\delta\tilde{v}$ and $\delta\tilde{w}$ are arbitrary by definition, which implies that they can be assigned any infinitesimal values, if these values are compatible with the system constraints such as its kinematical boundary conditions, Eq. (7) can be satisfied for all infinitesimal values of $\delta\tilde{v}$ and $\delta\tilde{w}$ if and only if

$$\varepsilon_m'-\frac{mR^2}{E}\ddot{\tilde{w}}=0 \tag{8}$$

for the axial deformation, and

$$\frac{r_x^2}{R^2}\tilde{v}^{iv}-\varepsilon_m\tilde{v}''-\varepsilon_m'\tilde{v}'-\varepsilon_m+\frac{mR^2}{E}\ddot{\tilde{v}}=\frac{\bar{\delta}(\theta)Q}{EA} \tag{9}$$

for the radial deformation; and at the boundaries $\theta=\pm\Theta$

$$\tilde{v}''=0. \tag{10}$$

In addition, the kinematical boundary conditions that

$$\tilde{w}=0 \quad \text{at } \theta=\pm\Theta \tag{11}$$

for the axial direction; and

$$\tilde{v}=0 \quad \text{at } \theta=\pm\Theta \tag{12}$$

for the radial direction need to be satisfied.

3. Static stability analysis

3.1. Nonlinear equilibrium

In order to use the principle of energy conservation to investigate the dynamic buckling of a shallow pin-ended arch under a suddenly applied central load with infinite duration, a knowledge of the static primary equilibrium path and of the secondary bifurcation equilibrium path of the arch under a static central load are essential. Hence, the static stability of a shallow pin-ended arch is first investigated here. For the static stability analysis, the displacements $\tilde{v}$ and $\tilde{w}$ are independent of time and so $\dot{\tilde{v}}=\ddot{\tilde{v}}=\dot{\tilde{w}}=\ddot{\tilde{w}}=0$. In this case, from Eq. (8), the membrane strain ε_m is a constant and can be written as

$$\varepsilon_m=-\frac{\bar{N}}{EA}, \tag{13}$$

where $\bar{N}$ is the internal axial compressive force in the arch.

By substituting Eqs. (8) and (13), the differential equation of equilibrium given by Eq. (9) becomes

$$\frac{\tilde{v}^{iv}}{\mu^2}+\tilde{v}''=\frac{\bar{\delta}(\theta)Q}{\bar{N}}-1, \tag{14}$$

where μ is a dimensionless axial force parameter defined by

$$\mu^2 = \frac{\bar{N}R^2}{EI_x}. \tag{15}$$

The solution of Eq. (14) can be obtained as

$$\tilde{v} = \frac{1}{\mu^2}\left\{1 - \frac{\cos(\mu\theta)}{\cos(\mu\Theta)} + \frac{\mu^2\Theta^2}{2} - \frac{\mu^2\theta^2}{2} + \frac{\bar{Q}}{\mu\Theta}[\tan(\mu\Theta)\cos(\mu\theta) - \mu\Theta + H(\theta)(\mu\theta - \sin(\mu\theta))]\right\}, \tag{16}$$

where the dimensionless load $\bar{Q}$ is given by

$$\bar{Q} = \frac{QR^2\Theta}{2EI_x} \tag{17}$$

and $H(\theta)$ is a step function that is given by

$$H(\theta) = \begin{cases} 1, & \theta > 0, \\ -1, & \theta < 0. \end{cases} \tag{18}$$

From Eq. (1), $\tilde{w}'$ can be expressed as

$$\tilde{w}' = \varepsilon_m + \tilde{v} - \tfrac{1}{2}\tilde{v}'^2. \tag{19}$$

Integrating Eq. (19) over the entire arch then produces

$$\int_{-\Theta}^{\Theta} \tilde{w}' \,\mathrm{d}\theta = \int_{-\Theta}^{\Theta} \left(\varepsilon_m + \tilde{v} - \frac{\tilde{v}'^2}{2}\right)\mathrm{d}\theta. \tag{20}$$

Because the axial displacement $\tilde{w} = 0$ at both pinned ends of the arch ($\theta = \pm\Theta$), the left side of Eq. (20) is given by

$$\int_{-\Theta}^{\Theta} \tilde{w}' \,\mathrm{d}\theta = \tilde{w}|_{-\Theta}^{\Theta} = 0. \tag{21}$$

Rewriting Eq. (13) as

$$\varepsilon_m = -\frac{\bar{N}}{EA} = -\frac{\bar{N}R^2}{EI_x}\frac{1}{R^2}\frac{I_x}{A} = -\frac{\mu^2 r_x^2}{R^2} \tag{22}$$

and substituting Eqs. (16) and (22) into Eq. (20) and then integrating Eq. (20) leads to the nonlinear equilibrium equation for shallow pin-ended arches as the transcendental equation

$$A_1\bar{Q}^2 + B_1\bar{Q} + C_1 = 0, \tag{23}$$

where the coefficients A_1, B_1 and C_1 are given by

$$A_1 = \frac{1}{4\mu^4\Theta^4}\left[\sec^2(\mu\Theta) - \frac{3\tan(\mu\Theta)}{\mu\Theta} + 2\right], \tag{24}$$

$$B_1 = \frac{1}{2\mu^4\Theta^4}\left[\frac{2\cos(\mu\Theta) - \mu\Theta\sin(\mu\Theta)}{\cos(\mu\Theta)^2} - 2\right], \tag{25}$$

$$C_1 = \left(\frac{\mu\Theta}{\lambda}\right)^2 + \frac{(\mu\Theta - \sin(\mu\Theta)\cos(\mu\Theta))}{4\mu^3\Theta^3\cos(\mu\Theta)^2} - \frac{1}{6} \tag{26}$$

in which the dimensionless arch geometric parameter λ is defined by

$$\lambda = \frac{R\Theta^2}{r_x} = \frac{S^2}{4r_xR} = \frac{\Theta S}{2r_x}. \tag{27}$$

3.2. Limit instability

A typical variation of the load and displacement obtained from Eqs. (16) and (23) for an arch with a geometric parameter $\lambda = 5$ is shown in Fig. 2. It is assumed that the arch is loaded in a displacement-

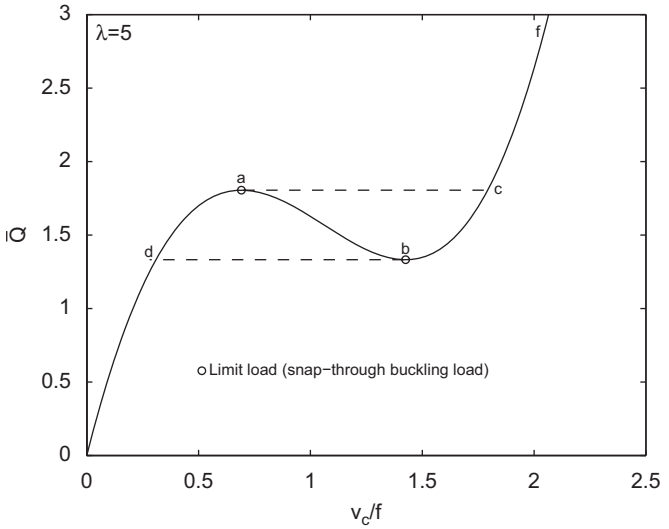

Fig. 2. Variation of load with displacement and limit instability.

controlled manner. As the displacement increases, the load increases along the stable equilibrium path $\circ a$ until the upper limit point a is reached. As the displacement continues to increase, the load decreases along the unstable equilibrium path ab until the lower limit point b is reached. As the displacement increases further, the load increases again along the stable equilibrium path bf. The loads corresponding to the upper and lower limit points are known as the upper and lower limit instability loads, respectively.

However, in practice, an arch is usually loaded in a load-controlled manner. When the load is increased further from the limit point a by an infinitesimal amount above the limit value, there is no adjacent equilibrium state and the only possible equilibrium state exists at a finite distance apart, i.e. at the state corresponding to the point c as shown in Fig. 2. Therefore, the arch snaps through from the equilibrium point a to the equilibrium point c, as indicated by the dashed lines in Fig. 2, which are not an equilibrium path. When the external load decreases, the arch follows the path fcb until the lower limit point b is reached. If the load is further decreased by an infinitesimal amount, there is no adjacent equilibrium state and the arch will snap-through to the equilibrium point d. Because of the snap-through phenomenon, the upper and lower limit instability loads are also known as the upper and lower snap-through buckling loads.

From Eqs. (17) and (23), the load Q can be expressed as an implicit function of the dimensionless axial force parameter μ as $F(Q,\mu)=0$. From calculus, the snap-through buckling load Q corresponding to the limit points a and b can be obtained by setting

$$\frac{\mathrm{d}Q}{\mathrm{d}\mu}=0, \tag{28}$$

which leads to an equilibrium equation for the snap-through buckling load $\bar{Q}_{\mathrm{st}}$ as

$$A_2\bar{Q}_{\mathrm{st}}^2+B_2\bar{Q}_{\mathrm{st}}+C_2=0, \tag{29}$$

where the coefficients A_2, B_2 and C_2 are given by

$$A_2=\frac{1}{8\mu^4\Theta^4}\left[7\sec^2(\mu\Theta)-\frac{15\tan(\mu\Theta)}{\mu\Theta}+8-\frac{2\mu\Theta\tan(\mu\Theta)}{\cos^2(\mu\Theta)}\right], \tag{30}$$

$$B_2=\frac{1}{4\mu^4\Theta^4}\left[\frac{8}{\cos(\mu\Theta)}-\frac{5\mu\Theta\tan(\mu\Theta)}{\cos(\mu\Theta)}-8-\frac{\mu^2\Theta^2}{\cos(\mu\Theta)}+\frac{2\mu^2\Theta^2}{\cos(\mu\Theta)}\right], \tag{31}$$

$$C_2=\frac{1}{8\mu^2\Theta^2}\left[\frac{3}{\cos^2(\mu\Theta)}-\frac{3\tan(\mu\Theta)}{\mu\Theta}-\frac{2\mu\Theta\tan(\mu\Theta)}{\cos^2(\mu\Theta)}\right]-\left(\frac{\mu\Theta}{\lambda}\right)^2. \tag{32}$$

The snap-through buckling load $\bar{Q}_{st}$ of an arch and the corresponding axial force parameter μ can be obtained by solving Eqs. (23) and (29) simultaneously. The buckling loads obtained from Eqs. (23) to (29) for the arch with $\lambda = 5$ are also shown in Fig. 2.

3.3. Bifurcation buckling

In addition to symmetric snap-through buckling, an arch may buckle in an antisymmetric bifurcation mode under a constant load from a prebuckling equilibrium configuration defined by $\{\tilde{v}, \tilde{w}\}$ to a buckled equilibrium configuration defined by $\{\tilde{v} + \tilde{v}_b, \tilde{w} + \tilde{w}_b\}$, where $\tilde{v}_b$ and $\tilde{w}_b$ are the buckling displacements in the radial and axial directions, respectively. By considering equilibrium in the prebuckled and buckled configurations, the differential equations of buckling equilibrium can be obtained as

$$\varepsilon'_{mb} = 0 \tag{33}$$

for the axial deformations; and

$$\frac{\tilde{v}_b^{iv}}{\mu^2} + \tilde{v}''_b = \frac{R^2 \varepsilon_{mb}}{r_x^2 \mu^2}(1 + \tilde{v}'') \tag{34}$$

for the radial deformations, where

$$\varepsilon_{mb} = \tilde{w}'_b - \tilde{v}_b + \tilde{v}'\tilde{v}'_b \tag{35}$$

is the membrane strain due to the buckling displacements, and where the second-order term $\tilde{v}_b'^2/2$ of the infinitesimal buckling deformation $\tilde{v}'_b$ is ignored.

The corresponding boundary conditions for buckling equilibrium are given by

$$\tilde{w}_b = 0 \quad \text{at } \theta = \pm\Theta \tag{36}$$

for the axial direction; and by

$$\tilde{v}_b = 0 \quad \text{and} \quad \tilde{v}''_b = 0 \quad \text{at } \theta = \pm\Theta \tag{37}$$

for the radial direction.

It can be obtained from Eq. (35) that

$$\tilde{w}'_b = \varepsilon_{mb} + \tilde{v}_b - \tilde{v}'\tilde{v}'_b. \tag{38}$$

Integrating Eq. (38) over the entire arch leads to

$$\frac{1}{2\Theta}\int_{-\Theta}^{\Theta} \tilde{w}'_b \, d\theta = \frac{1}{2\Theta}\int_{-\Theta}^{\Theta} (\varepsilon_{mb} + \tilde{v}_b - \tilde{v}'\tilde{v}'_b) \, d\theta. \tag{39}$$

From the boundary condition given by Eq. (36), the left side of Eq. (39) vanishes as

$$\frac{1}{2\Theta}\int_{-\Theta}^{\Theta} \tilde{w}'_b \, d\theta = \tilde{w}_b|_{-\Theta}^{\Theta} = 0. \tag{40}$$

On the right side of Eq. (39), the prebuckling radial displacements $\tilde{v}$ are symmetric and the prebuckling slopes $\tilde{v}'$ are antisymmetric while the buckling displacements $\tilde{v}_b$ are antisymmetric and the slopes $\tilde{v}'_b$ are symmetric. Therefore the terms $\tilde{v}_b$ and $\tilde{v}'\tilde{v}'_b$ are antisymmetric and so are odd functions of the angular coordinate θ, and their integration in the symmetric interval $[-\Theta, \Theta]$ also vanishes as

$$\frac{1}{2\Theta}\int_{-\Theta}^{\Theta} (\tilde{v}_b - \tilde{v}'\tilde{v}'_b) \, d\theta = 0. \tag{41}$$

Substituting Eqs. (40) and (41) into Eq. (39), and considering that from Eq. (33) the buckling membrane strain ε_{mb} is a constant leads to

$$\frac{1}{2\Theta}\int_{-\Theta}^{\Theta} \varepsilon_{mb} \, d\theta = \varepsilon_{mb} = 0, \tag{42}$$

which indicates the membrane strain ε_{mb} during buckling vanishes. By substituting $\varepsilon_{mb} = 0$ given by Eq. (42) into Eq. (34), the homogeneous differential equation for antisymmetric buckling of shallow arches is obtained as

$$\frac{\tilde{v}_b^{iv}}{\mu^2} + \tilde{v}_b'' = 0. \tag{43}$$

The general solution of Eq. (43) can be written as

$$\tilde{v}_b = E_1 \cos(\mu\theta) + E_2 \sin(\mu\theta) + E_3\theta + E_4. \tag{44}$$

Using the boundary conditions given by Eq. (37) leads to a group of four homogeneous algebraic equations for E_1, E_2, E_3 and E_4. The existence of non-trivial solutions for E_1–E_4 requires vanishing of the determinant of the coefficients matrix of the four equations, which leads to the characteristic equation that

$$\sin(\mu\Theta)\cos(\mu\Theta) = 0. \tag{45}$$

When the first factor of the characteristic equation (45) is equal to zero

$$\sin(\mu\Theta) = 0, \tag{46}$$

the lowest solution for $\mu\Theta$ is

$$\mu\Theta = \pi. \tag{47}$$

Substituting the solution $\mu\Theta = \pi$ into Eq. (23) leads to the equation for nonlinear antisymmetric bifurcation buckling as

$$A_3\bar{Q}_{bf}^2 + B_3\bar{Q}_{bf} + C_3 = 0, \tag{48}$$

where the coefficients A_3, B_3 and C_3 are given by

$$A_3 = \frac{3}{4\pi^4}, \quad B_3 = -\frac{2}{\pi^4}, \quad C_3 = \frac{3 - 2\pi^2}{12\pi^2} + \frac{\pi^2}{\lambda^2}. \tag{49}$$

The existence of real solutions of Eq. (49) for $\bar{Q}_{bf}$ requires $B_3^2 - 4A_3C_3 \geqslant 0$, which leads to

$$\lambda \geqslant \lambda_b = 7.97903, \tag{50}$$

where λ_b defines the lowest arch geometric parameter of an arch for antisymmetric bifurcation buckling. An arch with a geometric parameter $\lambda < \lambda_b$ does not buckle in an antisymmetric bifurcation mode.

However, $\lambda \geqslant \lambda_b$ does not guarantee the occurrence of bifurcation buckling because the bifurcation point may be located on the unstable equilibrium path after the instability limit. By letting the snap-through buckling load $\bar{Q}_{st}$ at $\mu\Theta = \pi$, obtained from Eq. (29), equal the bifurcation buckling load $\bar{Q}_{bf}$, obtained from Eq. (48), the value of the geometric parameter λ_{sb} that defines a switch between the snap-through and bifurcation buckling modes can be found as

$$\lambda_{sb} = 10.249505. \tag{51}$$

The variation of the loads and displacements obtained from Eqs. (16) and (48) for an arch with a geometric parameter $\lambda = 12$ is shown in Fig. 3. As the displacement increases, the load increases along the stable equilibrium path $\circ a$ until the upper bifurcation point a is reached. As the displacement continues to increase, the load decreases along the secondary bifurcation unstable equilibrium path ab until the lower bifurcation point b is reached. As the displacement increases further, the equilibrium bifurcates from the secondary bifurcation equilibrium path to the primary stable equilibrium path bf and the load again increases with an increase of the displacement along the stable equilibrium path bf.

The curve for primary equilibrium is also shown in Fig. 3. It can be seen that the upper limit instability load at the limit point a_s is higher than the upper bifurcation buckling load, while the lower limit instability load at the limit point b_s is lower than the lower bifurcation buckling load. Hence, the limit instability cannot occur.

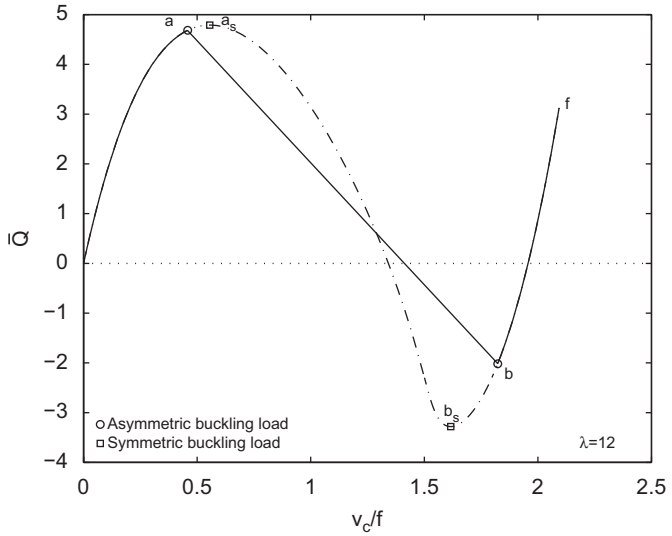

Fig. 3. Bifurcation asymmetric buckling.

3.4. Lowest buckling load

When the second factor of the characteristic equation (45) is equal to zero, i.e.

$$\cos(\mu\Theta) = 0, \tag{52}$$

the lowest solution for $\mu\Theta$ is

$$\mu\Theta = \frac{\pi}{2} \tag{53}$$

and the coefficient E_1 in the buckling displacement given by Eq. (44) does not vanish. Substituting $\mu\Theta = \pi/2$ into Eq. (44) leads to the buckling displacement $\tilde{v}_b$ as

$$\tilde{v}_b = E_1 \cos\frac{\pi\theta}{2\Theta}, \tag{54}$$

which is symmetric and does not lead to the vanishing of the buckling membrane strain $\varepsilon_{\mathrm{mb}}$ given by Eq. (35). Hence, the solution given by Eq. (53) does not correspond to bifurcation buckling, but corresponds to symmetric snap-through buckling.

Substituting the solution $\mu\Theta = \pi/2$ into Eq. (23) leads to the dimensionless buckling load $Q_{\mathrm{st}} = \pi/2$, which indicates that the upper and lower snap-through buckling loads are equal to each other when $\mu\Theta = \pi/2$.

The dimensionless central radial displacement $\tilde{v}_c$ corresponding to $\mu\Theta = \pi/2$ can be obtained from Eq. (16) by setting $\theta = 0$ as

$$\tilde{v}_{cs} = \lim_{\mu\Theta\to-\pi/2} v_c = \frac{(S)^2}{\pi^2 R^2}\left\{\frac{\pi^2}{8} - \frac{\pi}{2} + \frac{2+\pi}{\pi} + \frac{1}{6}\sqrt{\frac{6(24-18\pi^2+\pi^4+48\pi)}{\pi^2} - \frac{9\pi^4}{\lambda^2}}\right\}, \tag{55}$$

which is real if and only if

$$\frac{6(24-18\pi^2+\pi^4+48\pi)}{\pi^2} - \frac{9\pi^4}{\lambda^2} \geqslant 0 \tag{56}$$

from which

$$\lambda \geqslant \lambda_{\mathrm{sn}} = 3.9053. \tag{57}$$

When the geometric parameter of an arch $\lambda < \lambda_{\mathrm{sn}}$, in-plane buckling does not occur and the arch behaves in a similar way to a beam curved in elevation.

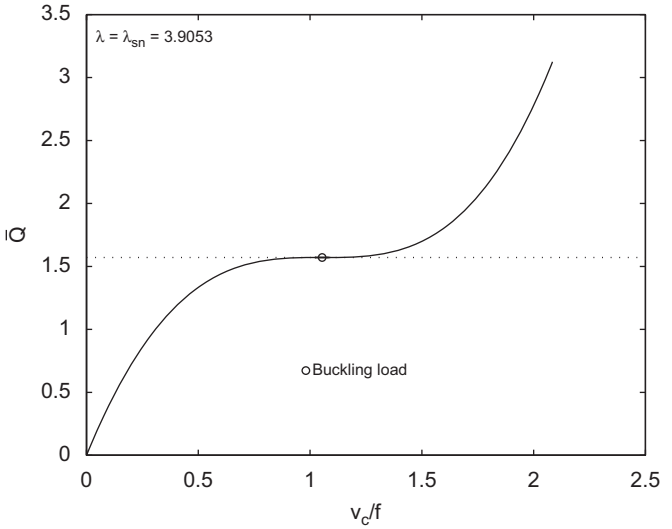

Fig. 4. The lowest buckling load.

The variation of the loads and displacements obtained from Eqs. (16) and (23) for the arch with a geometric parameter $\lambda_{sn} = 3.9053$ is shown in Fig. 4. This arch has the lowest buckling load $\bar{Q}_{st} = \pi/2$ and the upper and lower limit points merge into one. The total potential energies of the arch and load system at upper and lower buckling loads are equal to each other and so the lowest buckling load is also known as the energy buckling load [9,10].

The nonlinear static buckling under other loading and boundary conditions can be found in Pi et al. [12,21,22].

4. Dynamic stability

4.1. Energy criterion for dynamic instability

The dynamic solution from the equation of motion for the buckling analysis is much more difficult than using the equation of equilibrium for the static buckling analysis. At the same time, the complete dynamic solution is usually not needed for a dynamic buckling analysis, and what is needed is to find the critical states for the buckling. Herein, an effort will be devoted to finding the criterion that makes it possible to determine the dynamic buckling load without actually having to solve the equations of motion of the arch system. A dynamic load generally is one whose magnitude, direction, or point of application varies with time, and it is difficult to solve the dynamic buckling problem of a structure under a general dynamic load. This paper concentrates only on a sudden load with infinite duration, which is a special form of dynamic loading and is suddenly applied at $t = 0$. A suddenly applied load with infinite duration is also termed as a step load with infinite duration [1,3,4,16,18].

For clarity and without loss of generality, the one degree-of-freedom system of Simitses [4] shown in Fig. 5 is used to establish the criterion for the dynamic buckling of a conservative system under a suddenly applied horizontal load with infinite duration. The system consists of two rigid bars with the same length L pinned together and the other ends of the two bars are pin-ended or simply supported (Fig. 5). A mass m is attached to the pin-joint and a linear spring is connected to the pin-joint with the dimensions as shown in Fig. 5. The motion of the system under a sudden horizontal load Q can be described by the rotation angle θ. The system is assumed to have an initial angle θ_0. In this case, the dimensionless total potential energy $\bar{U}$ of the system is given by

$$\bar{U} = \frac{U}{kL^2} = (\sqrt{1+\sin\theta} - \sqrt{1+\sin\theta_0})^2 - \bar{Q}(\cos\theta_0 - \cos\theta), \tag{58}$$

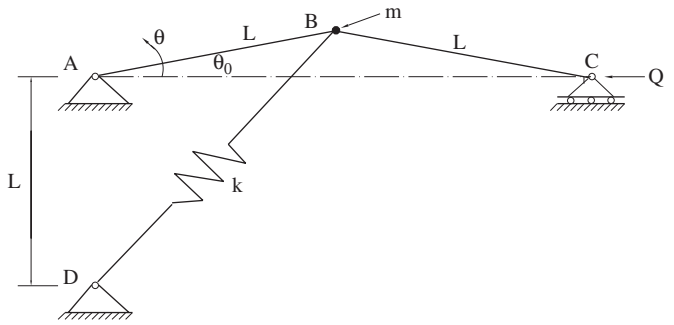

Fig. 5. Idealised system with one degree of freedom.

where U is the total potential energy of the system, the dimensionless load $\bar{Q}$ is given by $\bar{Q} = 2Q/kL$, and k is the stiffness of the spring (Fig. 5).

The static equilibrium points for the system can be obtained by setting

$$\frac{\mathrm{d}\bar{U}}{\mathrm{d}\theta} = 0, \tag{59}$$

which leads to the static equilibrium equation as

$$\bar{Q} = \frac{(\sqrt{1+\sin\theta} - \sqrt{1+\sin\theta_0})\cos\theta}{\sqrt{1+\sin\theta}\sin\theta}. \tag{60}$$

The variations of the dimensionless total potential energy $\bar{U}$ of the system with the rotation angle $(\theta - \theta_0)$ are shown in Fig. 6 for different values of the dimensionless load $\bar{Q}$.

Because the structure and sudden load with infinite duration form a conservative system, the total energy $\mathscr{E} = T + U$ of the system must satisfy the principle of energy conservation, which can be expressed in a dimensionless form as

$$\bar{\mathscr{E}} = \bar{T} + \bar{U} = \text{constant} \quad \text{with } \bar{\mathscr{E}} = \frac{\mathscr{E}}{kL^2}, \ \bar{U} = \frac{U}{kL^2}, \ \bar{T} = \frac{T}{kL^2}, \tag{61}$$

where the dimensionless kinetic energy of the system $\bar{T}$ is given by

$$\bar{T} = \frac{T}{kL^2} = \frac{m(L\dot{\theta})^2}{2kL^2} = \frac{1}{2}\dot{\theta}^2, \tag{62}$$

where T is the kinetic energy of the system, $\dot{\theta} = \mathrm{d}\theta/\mathrm{d}\tau$ is the dimensionless angular velocity of the system, and the dimensionless time parameter τ is defined by $\tau = t\sqrt{k/m}$.

It is assumed that before application of the load, the system is at rest without loading and so the constant in Eq. (61) is equal to zero, i.e.

$$\bar{\mathscr{E}} = \bar{T} + \bar{U} = 0. \tag{63}$$

From Eq. (62), the kinetic energy $\bar{T}$ is a positive definite function of the velocity $\dot{\theta}$. Hence, from the principle of energy conservation given by Eq. (63), motion of the system is possible when the total potential energy $\bar{U}$ is non-positive. For a dimensionless load $\bar{Q}$, two equilibrium positions can be found from Eq. (60): a stable equilibrium position A_i and an unstable equilibrium position B_i as shown in Fig. 6 where $\theta_0 = 0.006$ at $t = 0$. When the value of $\bar{Q}$ is small, for example $\bar{Q} = 0.4000$ or 0.4150, it can be seen that the total potential energy $\bar{U}$ corresponding to the unstable position B_1 and B_2 is positive. Hence, when the load $\bar{Q} = 0.4000$ or 0.4150 is suddenly applied, motion of the system corresponding to the unstable position B_1 or B_2 is impossible, and the system does not buckle dynamically but simply oscillates about a stable equilibrium position A_1 for $\bar{Q} = 0.4000$ or A_2 for $\bar{Q} = 0.4150$. As the dimensionless load $\bar{Q}$ increases, the total potential energy $\bar{U}$ of the system at the unstable equilibrium position B_i decreases. When the load $\bar{Q} = 0.4262$ is suddenly applied, the total potential energy $\bar{U}$ of the system at the unstable equilibrium position B_3 is equal to zero ($\bar{U} = 0$), and from the principle of energy conservation given by Eq. (63), the system can reach the unstable equilibrium position

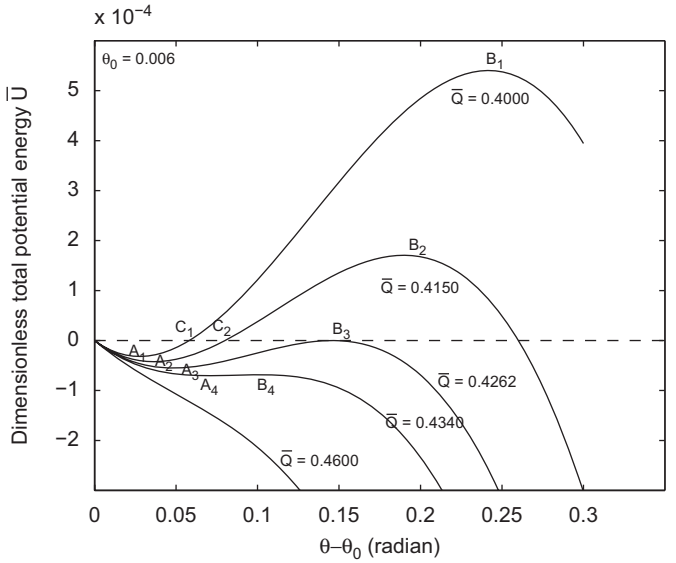

Fig. 6. Total potential energy and dynamic buckling: total potential energy.

(saddle) B_3 with zero kinetic energy. Subsequently, dynamic buckling of the system occurs at the load $\bar{Q} = 0.4262$. The dynamic buckling load $\bar{Q} = 0.4262$ of the system satisfies both the equilibrium equation (60) and the condition that the total potential energy $\bar{U}$ vanishes, i.e.

$$\bar{U} = 0. \tag{64}$$

Hence, the dynamic buckling load and the corresponding rotation θ can then be obtained by solving Eqs. (60) and (64) simultaneously as $\bar{Q}_d = 0.4262$ and $\theta = 0.1517602$ under the condition $\theta_0 = 0.006$.

If the load Q is slowly applied to the system, it can be considered as a static load and the system may buckle in a static mode. The static buckling load of the system needs to satisfy

$$\frac{\mathrm{d}^2\bar{U}}{\mathrm{d}\theta^2} = 0. \tag{65}$$

Solving Eqs. (60) and (65) simultaneously yields the static buckling load as $\bar{Q}_s = 0.4350$, which is higher than the dynamic buckling load $\bar{Q}_d = 0.4262$ of the system under a sudden loading with infinite duration.

4.2. Comparison with total energy-phase plane approach

To verify the reliability and efficiency of the energy criterion for dynamic buckling, the dynamic buckling load obtained by the energy criterion for the one degree-of-freedom system is compared with that obtained by a total energy-phase plane approach [2]. From Eqs. (64) to (62), Eq. (63) can be written as

$$\bar{\mathscr{E}} = \bar{T} + \bar{U} = \frac{1}{2}\dot{\theta}^2 + (\sqrt{1+\sin\theta} - \sqrt{1+\sin\theta_0})^2 - \bar{Q}(\cos\theta_0 - \cos\theta) = 0, \tag{66}$$

which is the equation of the phase trajectories for the motion of the system [4,16].

The typical trajectories of the phase-plane of $\dot{\theta}(\tau)$ ($\mathrm{d}\theta(\tau)/\mathrm{d}\tau$) and $\theta(\tau)$ for different values of the sudden load $\bar{Q}$ can be obtained from Eq. (66), and are shown in Fig. 7 where A_i are the stable equilibrium points and B_i are the unstable equilibrium points. It can be seen that when the load $\bar{Q} = 0.4000$ or 0.4150 is suddenly applied, the trajectories are closed and so an oscillatory periodic motion of the system about the near stable equilibrium point $A_i\,(i = 1, 2)$ occurs. The motion is bounded and the oscillations cannot reach the unstable equilibrium point $B_i\,(i = 1, 2)$. However, when the load $\bar{Q} = 0.4262$ is suddenly applied, the trajectory of the phase plane is through the corresponding unstable equilibrium point B_3 and becomes unbounded, and so unbounded motion, i.e. dynamic buckling of the system, is possible. When a load $\bar{Q} = 0.4340$ (>0.4262) is

suddenly applied, the trajectory of the phase plane is unbounded as shown in Fig. 7. Hence, from the trajectories of the phase plane, the critical load for dynamic buckling of the system is $\bar{Q}_d = 0.4262$, which is the same as that obtained from the energy criterion developed in Section 4.1.

It is known [4,20] that as the number of degrees of freedom increases the complexity of using the total energy-phase plane approach increases exponentially to the point of virtual impossibility when using the approach. Using this approach for the continuum, the phase space has to be reduced to finite-dimensional spaces.

4.3. Comparison with equations of motion approach

The equation of motion approach is probably the most commonly used approach [1–3,14,15]. Hence, the dynamic buckling load obtained by the energy criterion for the one degree-of-freedom system is also compared with that obtained by the equations of motion approach. The equation of motion for the one degree-of-freedom system (Fig. 5) can be obtained in a dimensionless form as

$$\ddot{\theta} + \cos\theta\left(1 - \frac{\sqrt{1+\sin\theta_0}}{\sqrt{1+\sin\theta}}\right) - \bar{Q}\sin\theta = 0. \tag{67}$$

Eq. (67) can be solved numerically under the initial conditions $\theta(\tau) = \theta_0$ and $\dot{\theta}(\tau) = 0$ at $\tau = 0$ using a numerical scheme such as the Runge–Kutta procedure. The results that are obtained for the dimensionless load $\bar{Q} = 0.4000$, 0.4150, 0.4261 and 0.4262 are shown in Fig. 8 as variations of $\theta(\tau)$ with the dimensionless time τ. It can be seen from Fig. 8 that when the load $\bar{Q} = 0.4000$, 0.4150 or 0.4261 is suddenly applied, the motion of the system is simply oscillatory. The oscillation takes place between the initial position $\theta_0 = 0.006$ and a maximum amplitude of $\theta(\tau)$ that is smaller than the maximum allowable value $\theta_{al} = \pi/2$. When the load $\bar{Q} = 0.4262$ is suddenly applied, the amplitude of the motion of the system becomes so large that escaping motion, i.e. dynamic buckling of the system, occurs as shown in Fig. 8.

Variations of the maximum response amplitude θ_{max} with the dimensionless load $\bar{Q}$ are shown in Fig. 9. It can be seen that there is large jump in the maximum amplitude θ_{max} at $\bar{Q} = 0.4262$. According to the Budiansky–Roth criterion [1], the dynamic buckling load is estimated to be $\bar{Q} = 0.4262$, which is the same as that obtained from the energy criterion in Section 4.1.

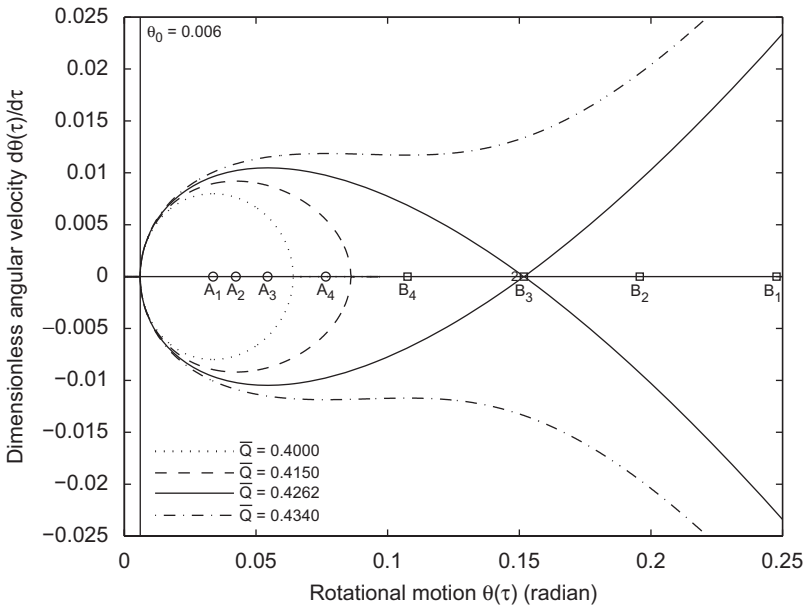

Fig. 7. Trajectories in the phase plane.

Although the equation of motion approach can be used with numerical methods to deal with a continuum subjected to a number of initial conditions by reducing the continuum to a multi-degree-of-freedom system, calculations in this approach require a large amount of time, which often makes its application very difficult for the analysis of multi-degree-of-freedom systems [17,20]. In addition, the accuracy of this approach often depends on the number of degrees of freedom of the reduced system and on the accuracy of the numerical method adopted [15].

4.4. Dynamic buckling load of shallow pin-ended arches

In this section, the energy criterion for the dynamic buckling developed and elucidated in Section 4.1 is applied to the dynamic buckling analysis of shallow pin-ended arches under a suddenly applied central load with infinite duration.

The dimensionless total potential energy $\bar{U}$ of the arch and load system can be obtained by substituting the solution for the radial displacement given by Eq. (16) into the dimensionless total potential energy expression

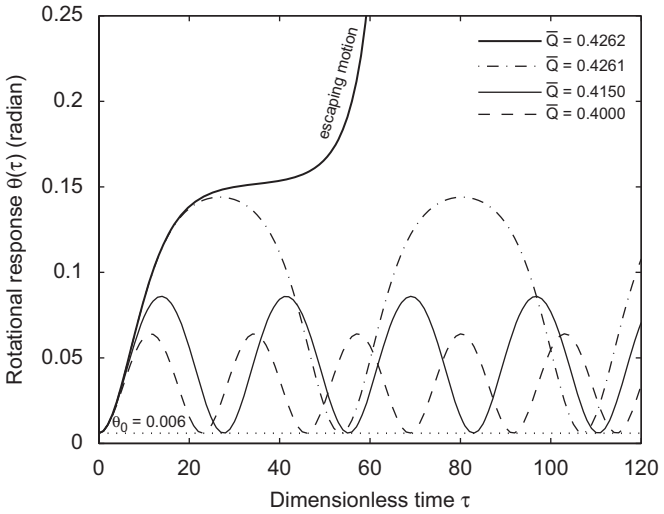

Fig. 8. Variations of the rotational response with dimensionless time.

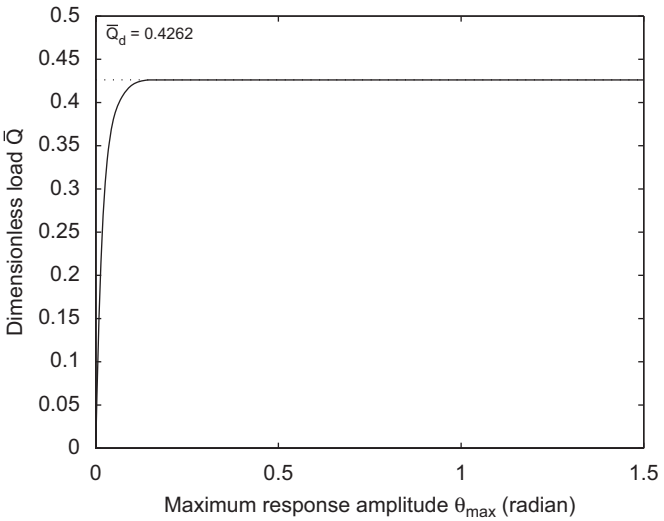

Fig. 9. Variations of the maximum amplitude θ_{max} with the dimensionless load $\bar{Q}$.

given by Eq. (4) and then integrating the expression as

$$\bar{U} = A_4\bar{Q}^2 + B_4\bar{Q} + C_4, \tag{68}$$

$$A_4 = \frac{r_x^2[\mu\Theta + 4\mu\Theta\cos^2(\mu\Theta) - 5\sin(\mu\Theta)\cos(\mu\Theta)]}{2\mu^3\Theta^2R^2\cos^2(\mu\Theta)}, \tag{69}$$

$$B_4 = \frac{r_x^2[4\cos(\mu\Theta) - 4\cos^2(\mu\Theta) - \mu^2\Theta^2\cos^2(\mu\Theta) - \mu\Theta\sin(\mu\Theta)]}{\mu^2\Theta R^2\cos^2(\mu\Theta)}, \tag{70}$$

$$C_4 = \frac{r_x^2\Theta}{R^2} + \frac{r_x^2\Theta}{2R^2\cos^2(\mu\Theta)} - \frac{3r_x^2\tan(\mu\Theta)}{2\mu R^2} + \frac{r_x^2\mu^2\Theta^3}{R^2}\left(\frac{\mu\Theta}{\lambda}\right)^2. \tag{71}$$

Before being subjected to the suddenly applied constant central load, the shallow arch is assumed to be free from loading and at rest. In this case, the principle of energy conservation given by Eq. (63) has to be satisfied. For a small load $\bar{Q}$, the dimensionless total potential energy $\bar{U}$ given by Eq. (68) corresponding to a stable equilibrium position may be non-positive and the kinetic energy imparted by the sudden load to the arch will induce oscillation of the arch about the stable equilibrium position. However, under the small load $\bar{Q}$, the dimensionless total potential energy $\bar{U}$ corresponding to an unstable equilibrium position is positive and so the motion of the arch to the unstable equilibrium position is impossible. As the value of the sudden load $\bar{Q}$ increases, the dimensionless total potential energy $\bar{U}$ to an unstable equilibrium position decreases until it becomes zero. From the principle of energy conservation, the arch can reach the unstable equilibrium position with zero kinetic energy, and dynamic buckling of the arch may therefore occur. Hence, vanishing of the total potential energy $\bar{U}$ of the arch

$$\bar{U} = A_4\bar{Q}^2 + B_4\bar{Q} + C_4 = 0 \tag{72}$$

is a necessary condition for the dynamic buckling of a shallow pin-ended arch under a sudden central load of infinite duration.

Because the dynamic buckling load corresponds to an unstable equilibrium position, it also needs to satisfy the equilibrium equation given by Eq. (23). The dynamic buckling load and the corresponding unstable equilibrium position can then be obtained by solving Eqs. (23) and (72) simultaneously. The equilibrium equation given by Eq. (23) describes the primary symmetric deformation of the arch and the load obtained is the upper dynamic buckling load. The total potential energy $\bar{U}$ may also vanish on the secondary bifurcation unstable equilibrium path. In this case, the lower dynamic buckling load can be obtained by substituting Eq. (47) into Eq. (72). Typical solutions for the upper and lower dynamic buckling loads are shown in Fig. 10 for an arch with a geometric parameter $\lambda = 12$ where the dimensionless load $\bar{Q}$ is defined by Eq. (17). In Fig. 10, the solid line is the primary equilibrium path under static loading, the dashed line is the secondary equilibrium path for bifurcation buckling, and the dot-dashed line represents the variation of the dimensionless load $\bar{Q}$ and axial force parameter $\mu\Theta$ for the condition of zero total potential energy ($\bar{U} = 0$). The intersection point d_u on the zero total potential energy curve and the unstable branch $a_s e b_s$ on the primary equilibrium path defines the upper dynamic buckling load while the intersection point d_l on the zero total potential energy curve and the secondary bifurcation equilibrium path ab defines the lower dynamic buckling load.

The variations of the dimensionless upper and lower dynamic buckling loads $QS^2/8EI_x$ with the arch geometric parameter λ are shown in Fig. 11. It can be seen that the dynamic buckling load increases with an increase of the arch geometric parameter. The variations of the static buckling loads $QS^2/8EI_x$ of the arches given by Eqs. (29) and (48) with the geometric parameter λ are also shown in Fig. 11. It can be seen that both the upper and the lower dynamic buckling loads are lower than the corresponding static buckling load.

To demonstrate the dynamic buckling behaviour, a typical dynamic buckling for a shallow pin-ended arch with a geometric parameter $\lambda = 6.5$ is shown in Figs. 12 and 13. Fig. 12 shows the static equilibrium path in terms of the dimensionless load $\bar{Q}$ and the dimensionless axial force parameter $\mu\Theta$, while Fig. 13 shows the equilibrium path in terms of the dimensionless load $\bar{Q}$ and the dimensionless central radial displacement v_c/f.

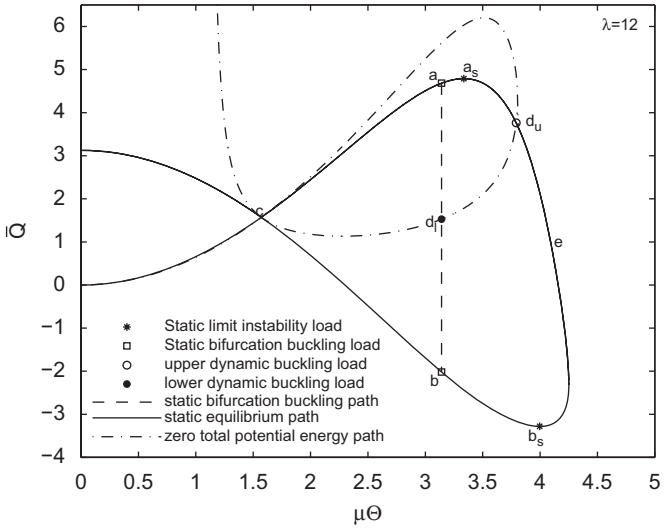

Fig. 10. Upper and lower dynamic buckling loads.

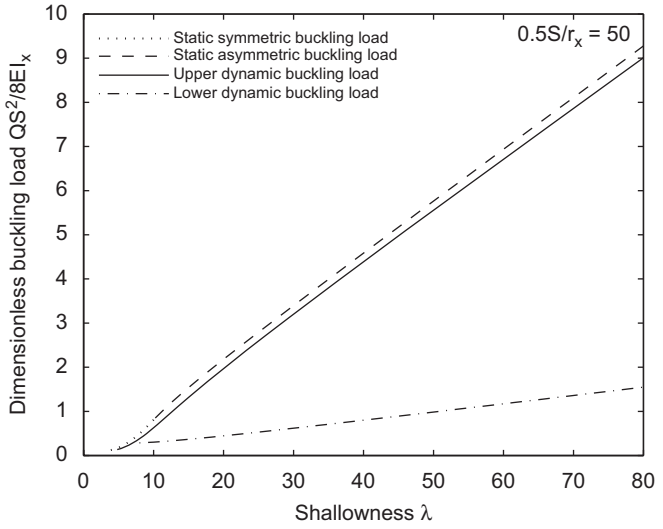

Fig. 11. Comparison of dynamic and static buckling loads for shallow arches.

Also shown in Figs. 12 and 13 are the dynamic buckling load, and the static buckling loads (limit instability load). The static buckling loads were obtained from Eqs. (23) to (29) while the dynamic buckling load was obtained from Eqs. (23) to (72).

When the suddenly applied load $\bar{Q} = 1.65$ is smaller than the dynamic buckling load, the dimensionless total potential energy $\bar{U}$ of the system corresponding to the stable equilibrium point s is obtained from Eq. (68) as $\bar{U} = -0.18492r_x^2\Theta/R^2$, which is negative, while the dimensionless total potential energy corresponding to the unstable equilibrium point u is $\bar{U} = 0.19127r_x^2\Theta/R^2$, which is positive. Hence, the sudden load will induce oscillation of the arch about the stable equilibrium position s and from the principle of energy conservation, the motion of the arch to the unstable equilibrium point u is impossible and so dynamic buckling cannot occur. However, when the suddenly applied load $\bar{Q}$ reaches the critical value $\bar{Q} = 1.840652$, the total potential energy $\bar{U}$ corresponding to the unstable equilibrium position d vanishes ($\bar{U} = 0$) and so the arch may reach the unstable equilibrium position d and buckle dynamically. Since under sudden loading, a displacement controlled loading regime is impossible, the arch snaps through from the unstable equilibrium point d to a

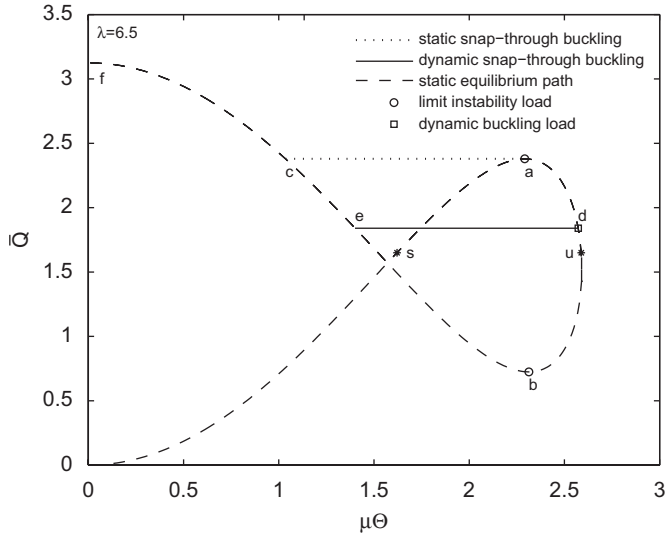

Fig. 12. Dynamic buckling of a shallow arch ($\bar{Q}$ against axial force parameter $\mu\Theta$).

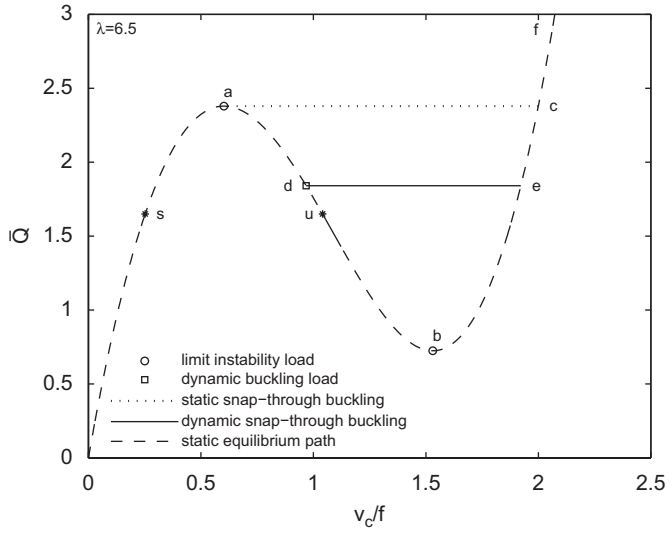

Fig. 13. Dynamic buckling of a shallow arch ($\bar{Q}$ against dimensionless central radial deflection v_c/f).

stable equilibrium point *e* which indicates the dynamic buckling of shallow arches under a sudden central load with infinite duration occurs in a snap-through mode.

From the static investigation, when the geometric parameter of an arch $\lambda < \lambda_{sn}$, the arch behaves as a beam with initial geometric imperfection. In this case, the dynamic buckling will not occur and the arch will oscillate about an equilibrium position. When the geometric parameter of an arch is in the range $\lambda_{sn} \leqslant \lambda \leqslant \lambda_b$, the arch does not buckle in a bifurcation mode. In this case, the upper dynamic buckling load of an arch is equal to its lower dynamic buckling load.

4.5. Effects of static preloading

In the previous discussion of dynamic buckling of a shallow pin-ended arch, the arch was assumed to be free from loading until the sudden load is applied. In most cases, an arch is subjected to some static loading before

the sudden load is applied, and the static load will influence the dynamic buckling of the shallow arch. Under a static central concentrated load Q_0, the corresponding axial force parameter μ_0 can be obtained from Eq. (23), and the dimensionless total potential energy $\bar{U}_0$ of the arch system can then be obtained by substituting μ_0 into Eq. (68) as

$$\bar{U}_0 = A_4^0 \bar{Q}_0^2 + B_4^0 \bar{Q}_0 + C_4^0 \tag{73}$$

with

$$A_4^0 = \frac{r_x^2[\mu_0\Theta + 4\mu_0\Theta\cos^2(\mu_0\Theta) - 5\sin(\mu_0\Theta)\cos(\mu_0\Theta)]}{2\mu_0^3\Theta^2R^2\cos^2(\mu_0\Theta)}, \tag{74}$$

$$B_4^0 = \frac{r_x^2[4\cos(\mu_0\Theta) - 4\cos^2(\mu_0\Theta) - \mu_0^2\Theta^2\cos^2(\mu_0\Theta) - \mu_0\Theta\sin(\mu_0\Theta)]}{\mu_0^2\Theta R^2\cos^2(\mu_0\Theta)}, \tag{75}$$

$$C_4^0 = \frac{r_x^2\Theta}{R^2} + \frac{r_x^2\Theta}{2R^2\cos^2(\mu_0\Theta)} - \frac{3r_x^2\tan(\mu_0\Theta)}{2\mu_0R^2} + \frac{r_x^2\mu_0^2\Theta^3}{R^2}\left(\frac{\mu_0\Theta}{\lambda}\right)^2. \tag{76}$$

In this case, the constant C in the principle of energy conservation given by Eq. (61) is equal to the dimensionless total potential energy $\bar{U}_0$ of the preloaded arch system and so the principle of energy conservation can be written in a dimensionless form as

$$\bar{U} + \bar{T} = \bar{U}_0, \tag{77}$$

where the dimensionless total potential energy $\bar{U}$ is given by Eq. (68).

The criterion for dynamic buckling of the statically preloaded arch can then be expressed as

$$\bar{U} - \bar{U}_0 = 0. \tag{78}$$

Simultaneously solving Eqs. (23) and (78) yields the dynamic buckling load $\bar{Q}_d$ of an arch with a static central pre-applied load $\bar{Q}_0$. To show the effects of pre-applied static load on the dynamic buckling, the variations of the dimensionless upper dynamic buckling loads $\bar{Q}_d$ and $\bar{Q}_d + \bar{Q}_0$ with the pre-applied static load $\bar{Q}_0$ for an arch with a geometric parameter $\lambda = 20$ are shown in Fig. 14. Also shown in Fig. 14 are the static buckling loads obtained from Eqs. (29) and (48) and the dynamic buckling load obtained from Eqs. (23) to (72). It can be seen that the static preloading decreases the dynamic buckling loads $\bar{Q}_d$, but increases the total loads $\bar{Q}_0 + \bar{Q}_d$ at the occurrence of dynamic buckling. It can also be seen that the total loads $\bar{Q}_0 + \bar{Q}_d$ are lower than

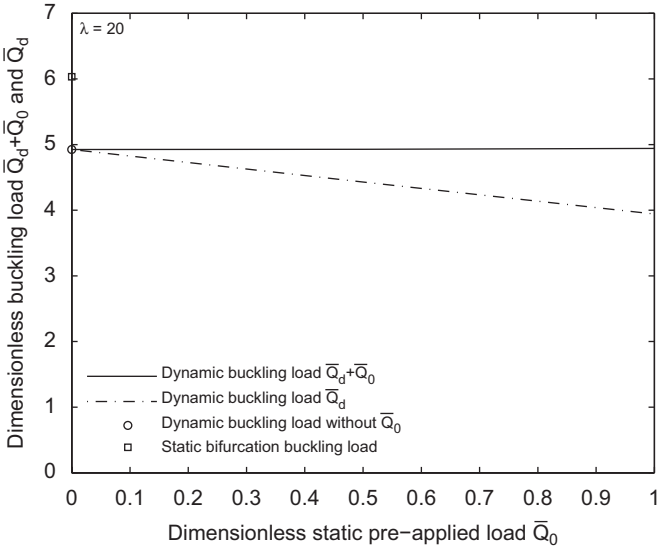

Fig. 14. Effects of static preloading on dynamic buckling of a shallow arch.

the corresponding static buckling loads. As expected, when the pre-applied static load is higher than the static buckling load of the arch, static buckling of the arch will occur under this static load.

5. Conclusions

This paper has used a method based on the principle of energy conservation to establish the criterion for the in-plane dynamic buckling of shallow pin-ended circular arches that are subjected to a central radial load applied suddenly with infinite duration. The merit of the criterion is that it can determine the critical buckling load without the need to solve the equations of motion of the arch system. The exact total potential energy, and the exact primary equilibrium and secondary bifurcation equilibrium paths have been obtained, which are essential for the dynamic buckling analysis based on the principle of energy conservation. Analytical solutions for the upper and lower dynamic buckling loads of shallow pin-ended arches under the sudden central constant load with infinite duration have been obtained. Because they are based on the exact total potential energy and equilibrium paths, the solutions for the dynamic buckling loads are accurate. It has been found that the dynamic buckling load for a pin-ended arch increases with an increase of the arch geometric parameter and that when the geometric parameter of an arch is less than the lowest geometric parameter ($\lambda < \lambda_b$) for antisymmetric bifurcation buckling, the upper and lower dynamic buckling loads are equal to each other. It has been found that the dynamic buckling load of a shallow pin-ended arch due to the sudden loading is lower than its static counterpart. The effect of a static preloading on the dynamic buckling of a shallow pin-ended arch has also been investigated. It has been found that the pre-applied static load decreases the dynamic buckling load, but increases the total of the pre-applied load and the dynamic buckling load.

Acknowledgements

This work has been supported by the Australian Research Council through Discovery Projects, and an Australian Research Council Federation Fellowship awarded to the second author.

References

[1] B. Budiansky, R.S. Roth, Axisymmetric dynamic buckling of clamped shallow spherical shells, Collected Papers on Instability of Shell Structures, NASA TN D-1510, 1962.
[2] B. Budiansky, J.W. Hutchinson, Dynamic buckling of imperfection-sensitive structures, *Proceedings XI International Congress of Applied Mechanics*, Munich, 1964.
[3] C.S. Hsu, Stability of shallow arches against snap-through under timewise step loads, *Journal of Applied Mechanics* 35 (1) (1968) 31–39.
[4] G.J. Simitses, *Dynamic Stability of Suddenly Loaded Structures*, Springer, New York, 1990.
[5] D.L.C. Lo, E.F. Masur, Dynamic buckling of shallow arches, *Journal of the Engineering Mechanics Division ASCE* 102 (EM3) (1976) 901–917.
[6] W.E. Gregory Jr., R.H. Plaut, Dynamic stability boundaries for shallow arches, *Journal of the Engineering Mechanics Division ASCE* 108 (EM6) (1982) 1036–1050.
[7] G. Herrmann, *Dynamic Stability of Structures*, Pergamon Press, Oxford, 1967.
[8] M.T. Donaldson, R.H. Plaut, Dynamic stability boundaries of a sinusoidal shallow arch under pulse loads, *AIAA Journal* 21 (3) (1983) 469–471.
[9] A. Gjelsvik, S.R. Bodner, Energy criterion and snap-through buckling of arches, *Journal of the Engineering Mechanics Division ASCE* 88 (EM5) (1962) 87–134.
[10] H.L. Schreyer, E.F. Masur, Buckling of shallow arches, *Journal of the Engineering Mechanics Division ASCE* 92 (EM4) (1966) 1–17.
[11] F.F. Dickie, P. Broughton, Stability criteria for shallow arches, *Journal of the Engineering Mechanics Division ASCE* 97 (EM3) (1971) 951–965.
[12] Y.L. Pi, M.A. Bradford, B. Uy, In-plane stability of arches, *International Journal of Solids and Structures* 39 (1) (2002) 105–125.
[13] M.A. Bradford, B. Uy, Y.L. Pi, In-plane stability of arches under a central concentrated load, *Journal of Engineering Mechanics ASCE* 128 (7) (2002) 710–719.
[14] H. Matsunaga, In-plane vibration and stability of shallow circular arches subjected to axial forces, *International Journal of Solids and Structures* 33 (4) (1996) 469–482.
[15] C.S. Huang, K.Y. Nieh, M.C. Yang, In-plane free vibration and stability of loaded and shear deformable circular arches, *International Journal of Solids and Structures* 40 (22) (2003) 5865–5886.

[16] A.N. Kounadis, J. Raftoyiannis, J. Mallis, Dynamic buckling of an arch model under impact loading, *Journal of Sound and Vibration* 134 (2) (1989) 193–202.
[17] J. Levitas, J. Singer, T. Weller, Global dynamic stability of a shallow arch by Poincarè-like simple cell mapping, *International Journal of Non-Linear Mechanics* 32 (2) (1997) 411–424.
[18] O.C. Pinto, P.B. Goncalves, Non-linear control of buckled beams under step loading, *Mechanical Systems and Signal Processing* 14 (6) (2000) 967–985.
[19] A.N. Kounadis, C.J. Gantes, V.V. Bolotin, Dynamic buckling loads of autonomous potential system based on the geometry of the energy surface, *International Journal of Engineering Science* 37 (1999) 1611–1628.
[20] A.N. Kounadis, C.J. Gantes, I.G. Raftoyiannis, A geometric approach for establishing dynamic buckling load of autonomous potential *N*-degree-of-freedom systems, *International Journal of Non-Linear Mechanics* 39 (2004) 1635–1646.
[21] Y.-L. Pi, M.A. Bradford, F. Tin-Loi, Nonlinear analysis and buckling of elastically supported circular shallow arches, *International Journal of Solids and Structures* 44 (7–8) (2007) 2401–2425.
[22] Y.-L. Pi, M.A. Bradford, F. Tin-Loi, Nonlinear in-plane buckling of rotationally restrained shallow arch under a central concentrated load, *International Journal of Non-Linear Mechanics* 43 (1) (2008) 1–17.